Title
RADIATION FIELD INSIDE A THICK CONCRETE SHIELD FOR 6.2 -BeV INCIDENT PROTONS

Authors
Smith, Alan R.
McCaslin, Joseph B.
Pick, Michael A.

Publication Date
1964-09-18

UCRL-11331

University of California

Ernest O. Lawrence Radiation Laboratory

RADIATION FIELD INSIDE A THICK CONCRETE SHIELD FOR 6.2-BeV INCIDENT PROTONS

Berkeley, California

UCRL-11331

UNIVERSITY OF CALIFORNIA
Lawrence Radiation Laboratory
Berkeley, California

AEC Contract No. W-7405-eng-48

RADIATION FIELD INSIDE A THICK CONCRETE SHIELD FOR 6.2-BeV INCIDENT PROTONS

Alan R. Smith, Joseph B. McCaslin,
and Michael A. Pick

September 18, 1964

RADIATION FIELD INSIDE A THICK CONCRETE SHIELD FOR 6.2-BeV INCIDENT PROTONS

Alan R. Smith, Joseph B. McCaslin,
and Michael A. Pick*

Lawrence Radiation Laboratory
University of California
Berkeley, California

September 18, 1964

ABSTRACT

We describe an investigation of some characteristics of the radiation field inside a massive shield of ordinary concrete when such a structure is bombarded by a sharply focussed beam of 6.2-BeV protons. For our purpose, the external proton beam from the Berkeley Bevatron is directed onto one face of the shield array. This array permits study of the radiation field to depths of 24 ft along the beam axis, and laterally to distances of 10 ft off-axis.

Attenuation measurements obtained during the experiment are presented here. Complete sets of lateral activity profiles were obtained with gold foils (thermal-neutron flux), aluminum discs (flux greater than 7 MeV), and carbon scintillators (flux greater than 20 MeV). Several transformations of the data are shown in an effort to clarify properties of the radiation field as viewed by these three detectors.

Such information should be of immediate value to shield design at particle accelerators in the multi-BeV energy range; therefore we present the attenuation measurements now, and do not delay until data processing and analysis from other aspects of the experiment are complete. These aspects include measurement of fast-neutron flux, fast-neutron spectra, and induced activation of several important accelerator construction materials; the results will be reported as they become available.

---

* Members of the Health Physics Department, Lawrence Radiation Laboratory.

DESCRIPTION OF EXPERIMENT

Our experiment concerns the shielding of high-energy particle accelerators. For this purpose, we use the 6-BeV external proton beam produced by the Bevatron. Figure 1 shows a plan view of the experimental setup. The primary proton beam enters from the right along a shielded channel; this channel narrows to a 2- by 2-ft cross-section area about 8 ft ahead of the shield array. A thin plastic scintillator is located at the front of the narrow channel and is viewed by closed-circuit television. The position and size of the beam spot are continuously observed in this fashion; correct beam alignment is verified by reference to a grid scribed on the scintillator. The beam spot was usually no greater than 2 in. in extent as viewed by the scintillator-television system.

The shield array consists of ordinary concrete in block form, and is 28 ft thick along the beam line, 22 ft wide, and 18 ft high. Slots provide access to the beam line at 4-ft intervals. Several special thin blocks are seen at the front of the array, to allow more detailed study in this region; access is from the top for these positions. Rows of blocks are separated by 3-in.-wide gaps to allow insertion of detectors. All portions of these gaps, except the 18-in.-high slots actually used for detector placement, are filled with gypsum wallboard, to minimize air spaces along which neutrons could scatter or diffuse.

Figure 2, a photograph of the working face of the array, gives some idea of the actual setup and the manner in which it was used. A wooden trough, loaded with detectors, has just been inserted in one of the slots; all detectors were positioned for exposure in this fashion.

The principal detectors are the activation-threshold type. In such a detector, one observes an integrated response that can be produced only by neutrons (or protons) whose energy is greater than some "threshold" value. When several elements are so used, each having a different threshold energy, we can obtain information related to behavior of different energy groups in the experimental constraints. Ultimately, one may be able to construct a neutron (or proton) spectrum from these data.

Figure 3 shows a set of detectors arranged in the wooden troughs, ready for exposure at beam-axis positions in the shield array. Among the elements employed are: aluminum, carbon, cobalt, copper, iodine, iron,

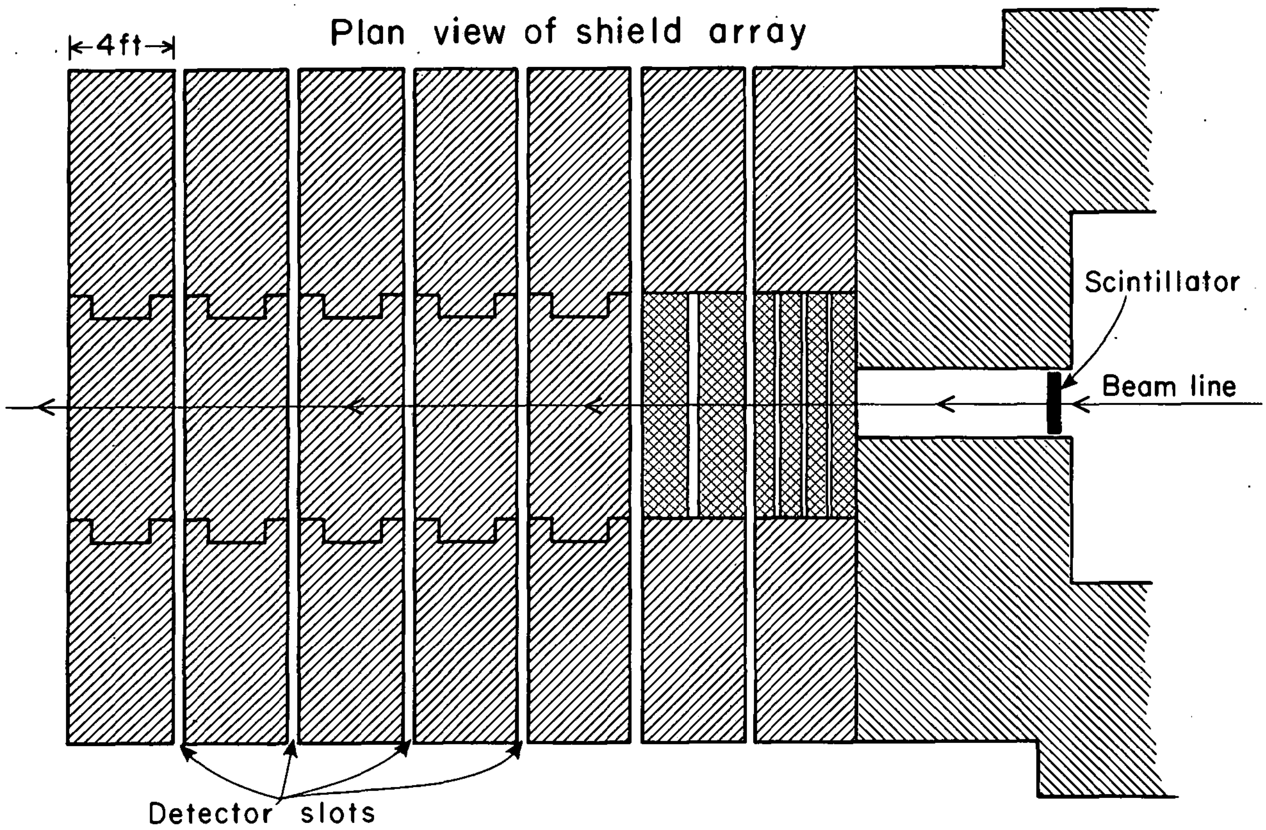

MUB-3055

Fig. 1. Plan view of shield array.

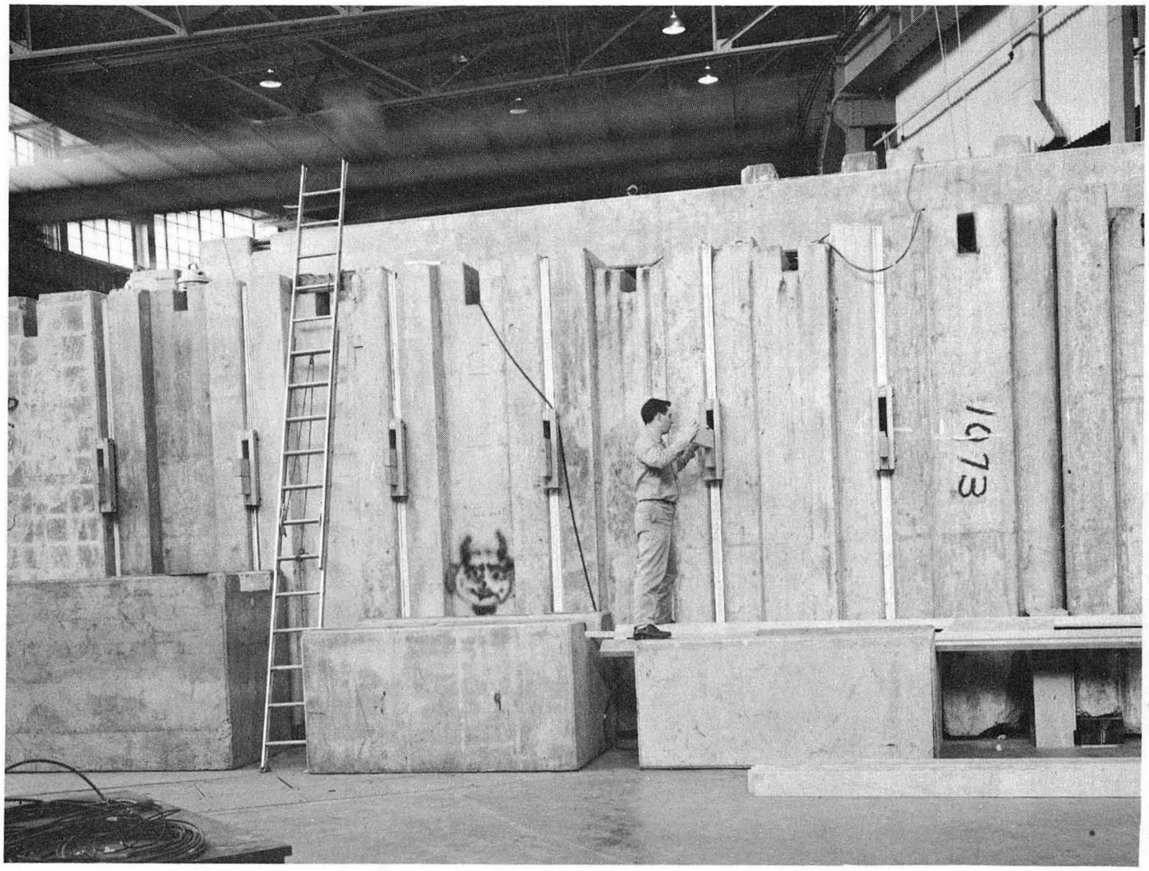

ZN-4498

Fig. 2. Working face of shield array.

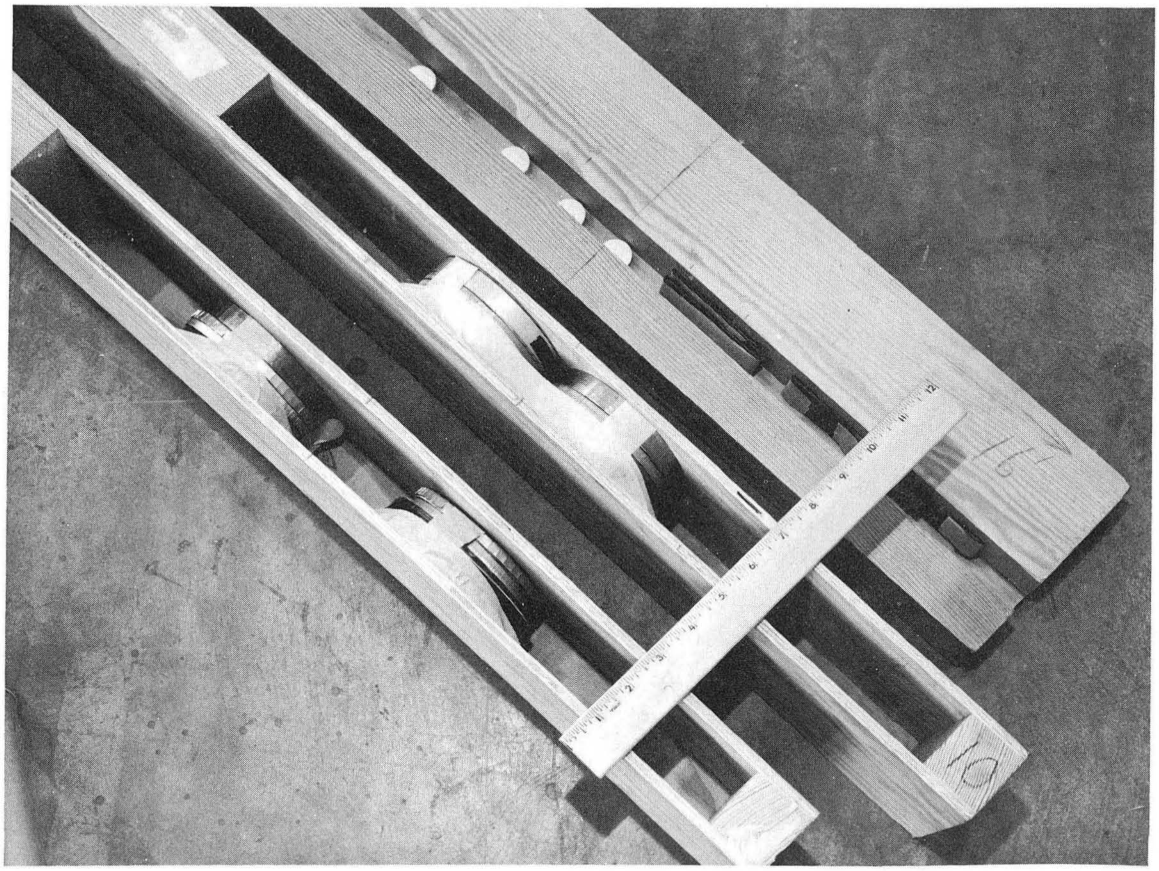

ZN-4499

Fig. 3. Detectors positioned in wooden troughs.

magnesium, nickel, and titanium. These materials are used in the form of 4-in.-diam discs, of thicknesses between 1/32 and 1 in. With one exception we observe the gamma-ray activity of radioisotopes produced during irradiations; this exception is carbon. Here we use carbon in the form of a plastic scintillator, and detect the positron decay directly inside the scintillator. From all other materials, we obtain multichannel gamma-ray spectra with a sodium iodide crystal scintillation spectrometer. Spectra are studied during decay of the various isotopes until we can obtain quantitative results for each isotope of importance.

ATTENUATION MEASUREMENTS

The shield structure existed for two months, and during most of that time it served as the external-beam backstop for a physics experiment. Much of the period was suitable for our purposes, and it was at such times that we developed a series of attenuation profiles within the array. Gold foils, aluminum discs, and carbon scintillators were so employed, to provide information about three neutron-energy groups. Detector activities were observed at every 4-ft depth, laterally from the beam axis to the shield's edge at 1-ft intervals. From these data we have constructed detailed radiation profiles for all positions inside the shield array, as viewed by these three detectors. Most exposures were performed when the external-proton-beam intensity ranged between 10^{10} and 10^{11} protons per second; exposures varied in length from about one to several hundred minutes. Careful attention was given to insure that each exposure provided sufficient normalization data so that all results could be properly related within a single comprehensive framework.

PRESENTATION FORMAT

Essentially all the useful data presented here is in graphical form. In an effort to enhance the value of this graphical information, Figs. 4 through 8 are reproduced full size; that is, one can retrieve detailed numerical values by simply tracing our curves on standard 8 1/2" × 11" sheets of graph paper. Figures 4, 5, and 8 are drawn on semi-logarithmic paper, with 7 cycles vertically and 10 divisions per inch horizontally, Keuffel and Esser type 359-96, or equivalent. Figures 6 and 7 are drawn on Cartesian-coordinate

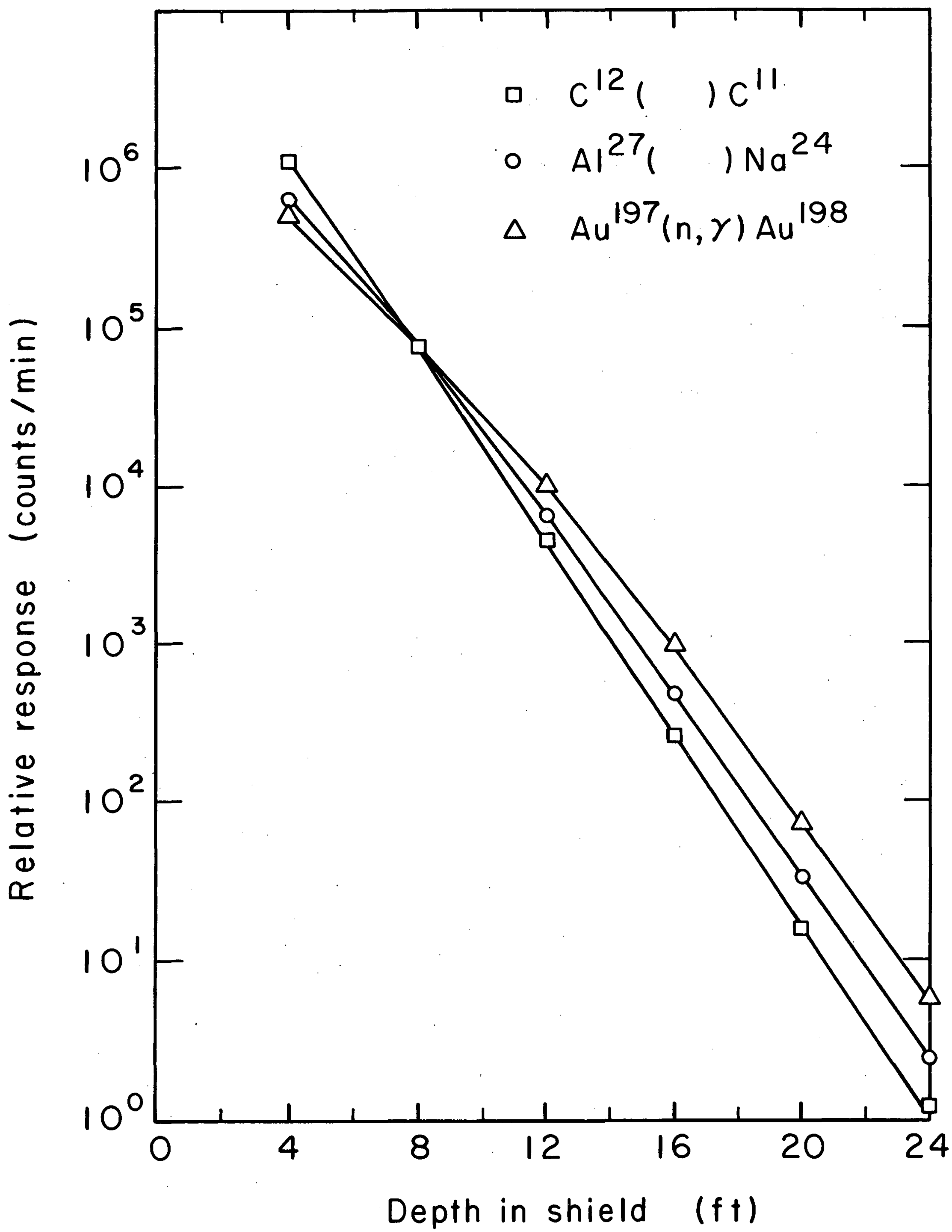

Fig.4 Beam-axis attenuation profiles for carbon, aluminum, and gold

MUB-3056 -A

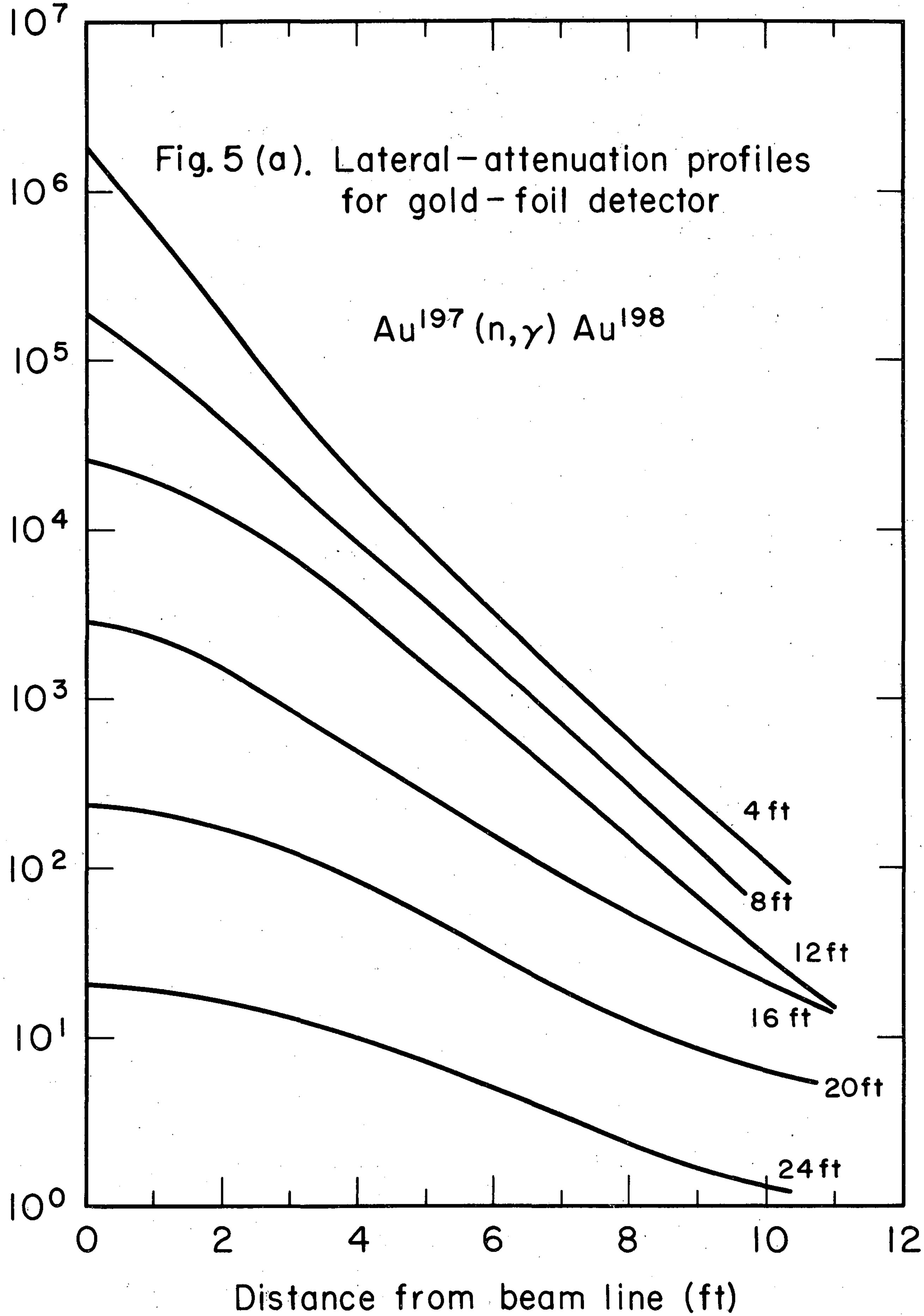

Fig. 5 (a). Lateral-attenuation profiles for gold-foil detector
$Au^{197}(n,\gamma)Au^{198}$
Relative response (counts/min)
Distance from beam line (ft)
4 ft
8 ft
12 ft
16 ft
20 ft
24 ft

MUB-4044

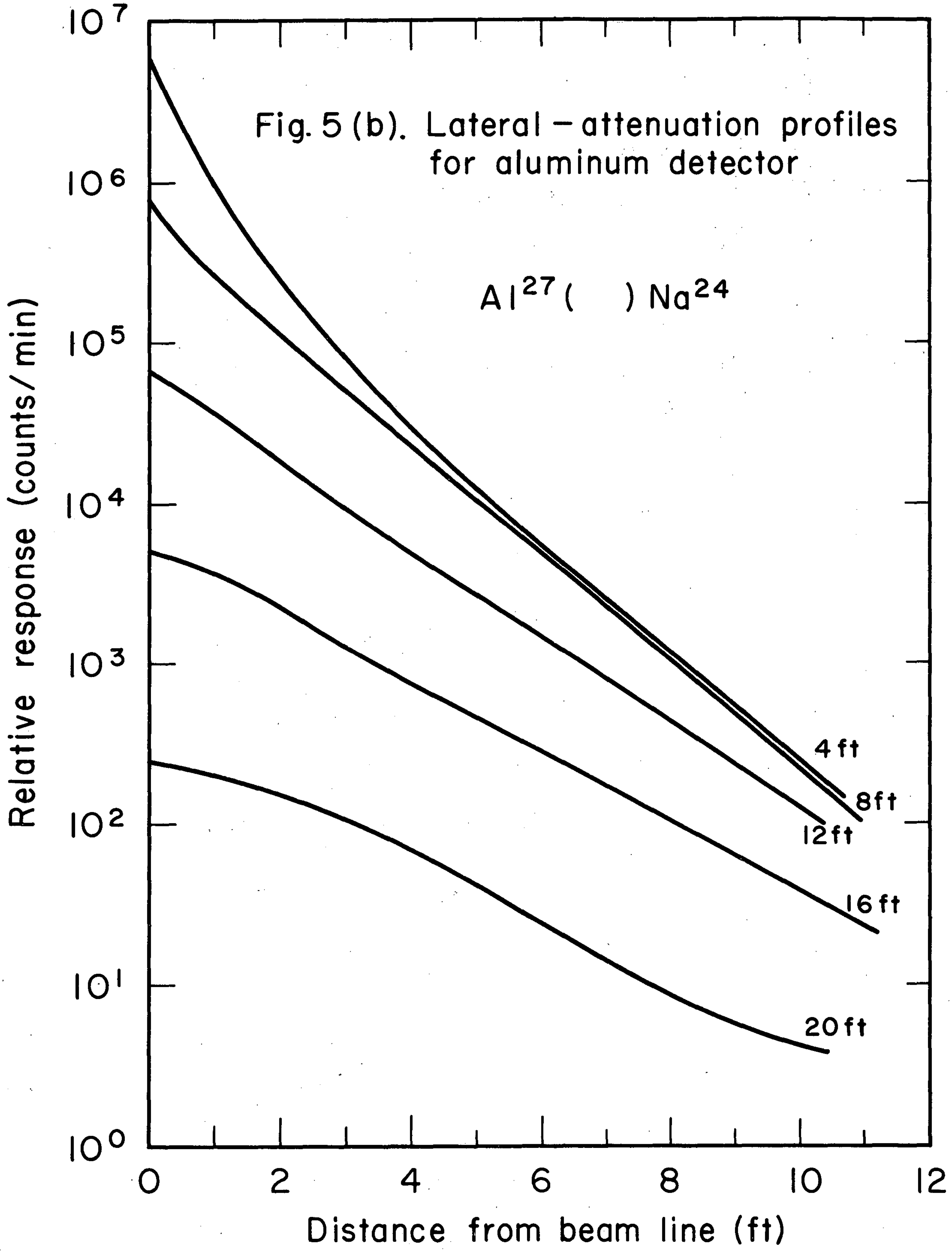
Fig. 5 (b). Lateral – attenuation profiles for aluminum detector
Al27( ) Na24
4 ft
8 ft
12 ft
16 ft
20 ft
Relative response (counts/min)
Distance from beam line (ft)
10^7
10^6
10^5
10^4
10^3
10^2
10^1
10^0
0
2
4
6
8
10
12

MUB-4045

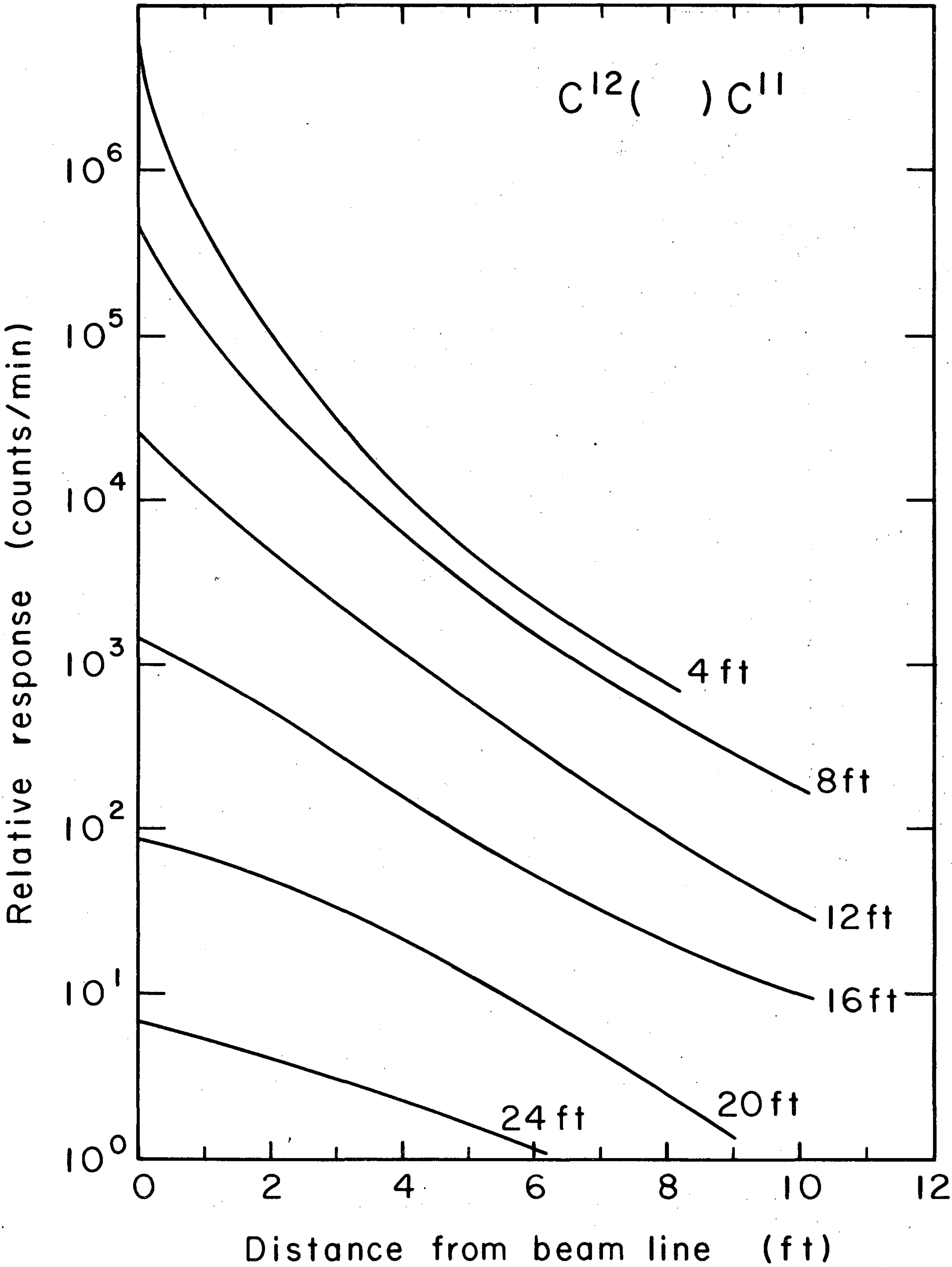

Fig. 5 (c). Lateral-attenuation profiles for carbon detector

MUB-3057 A

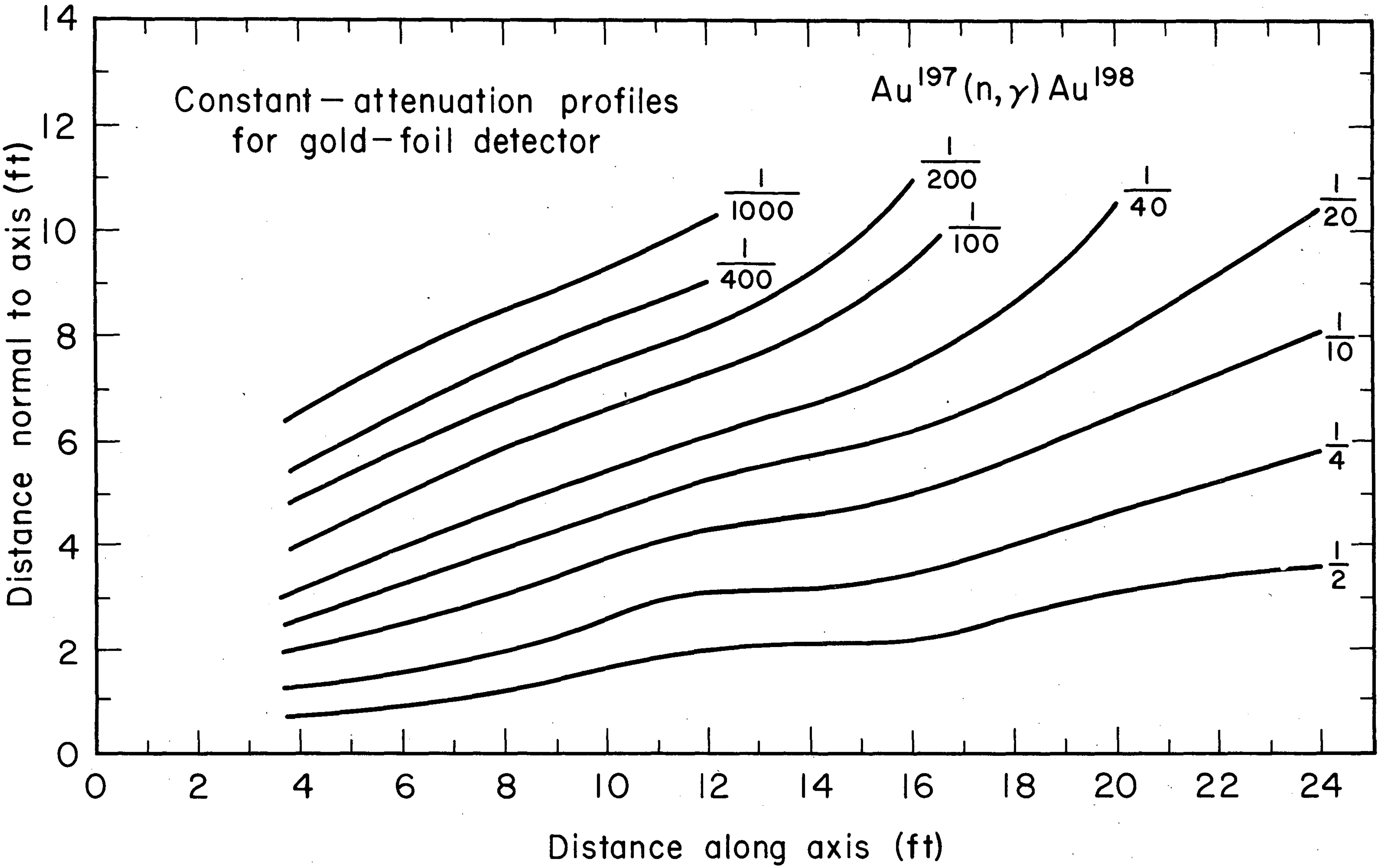

Fig. 6 (a)

MUB-4046

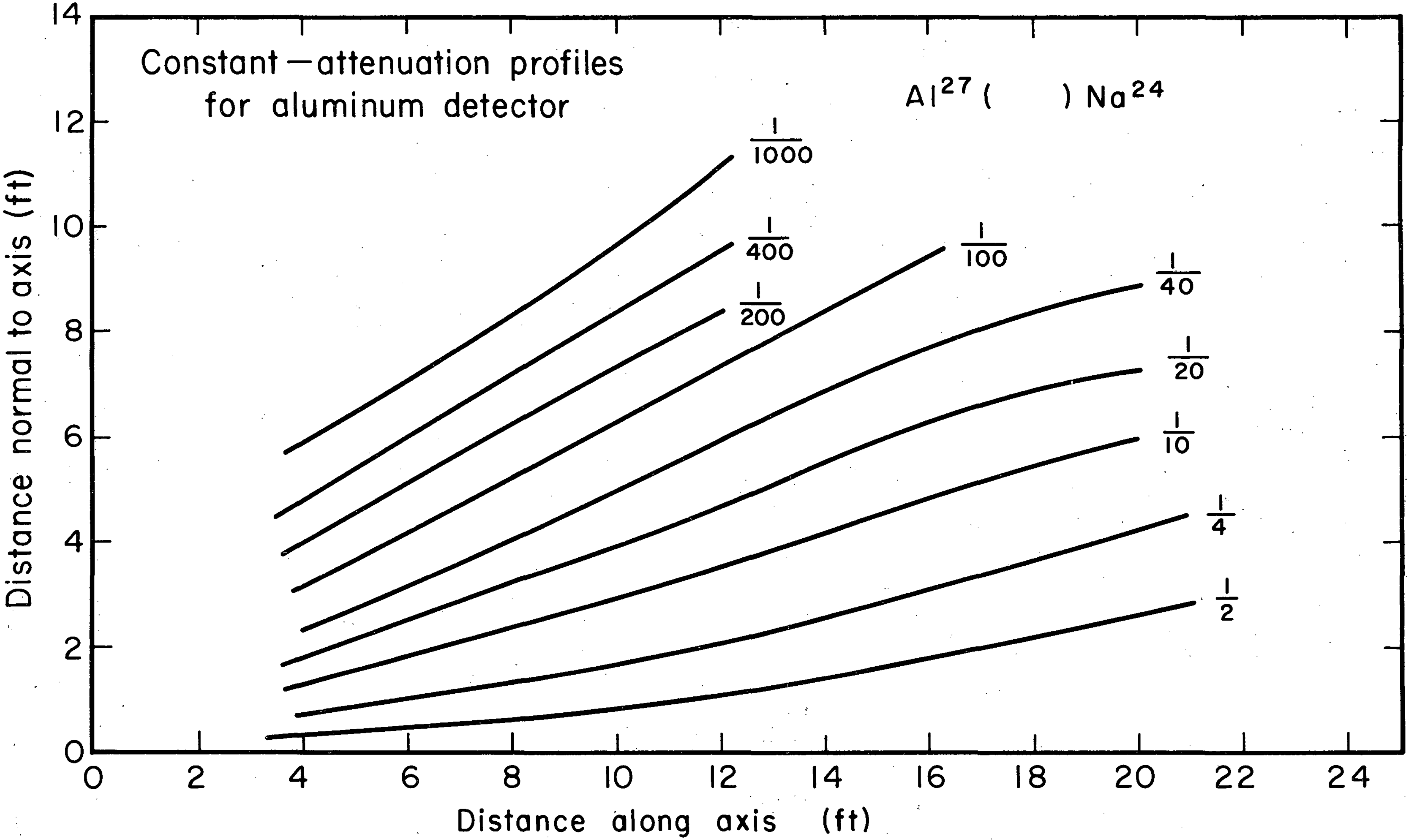

Fig. 6 (b)

MUB-4047

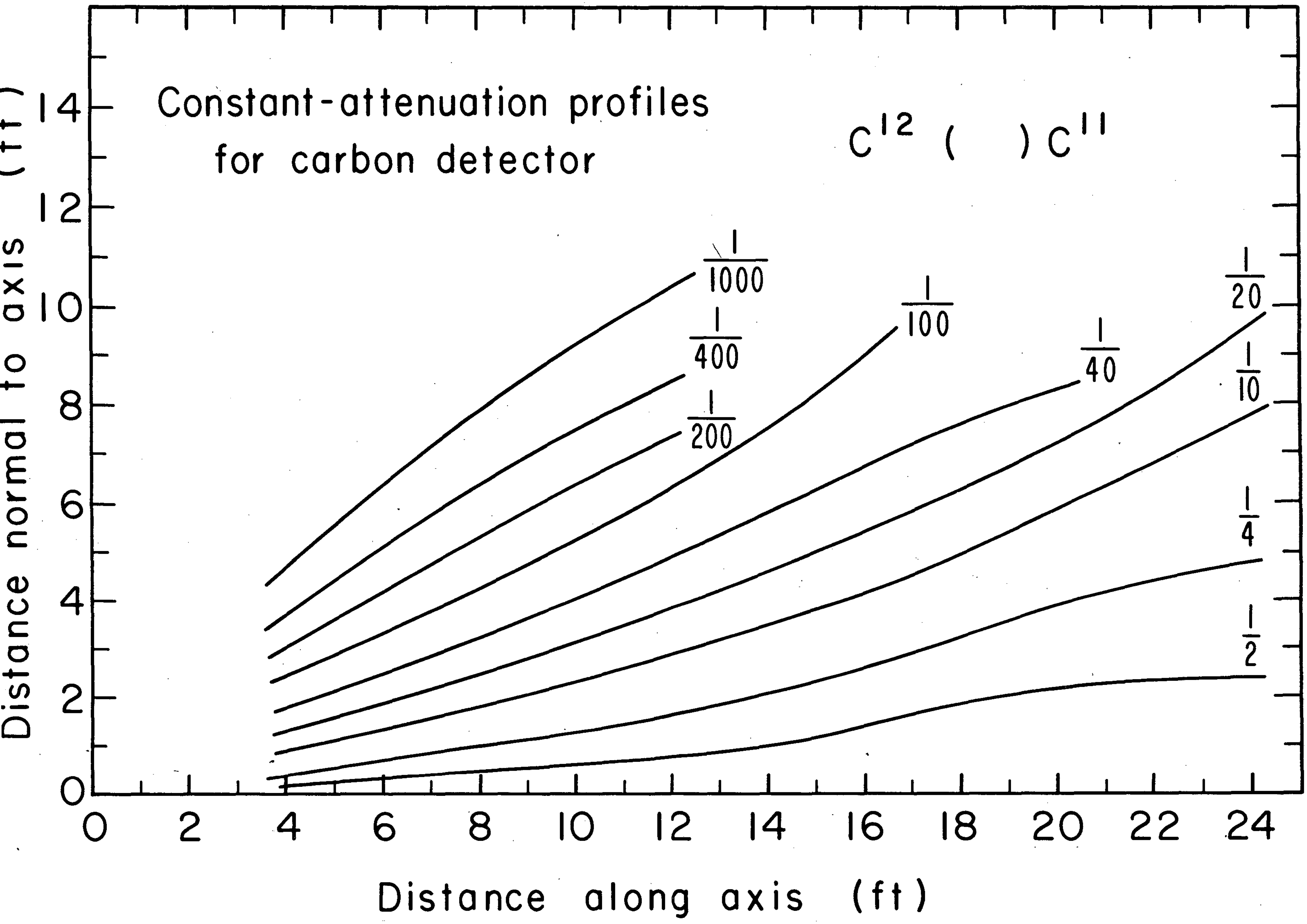

Fig. 6(c)

MUB-3058 -A

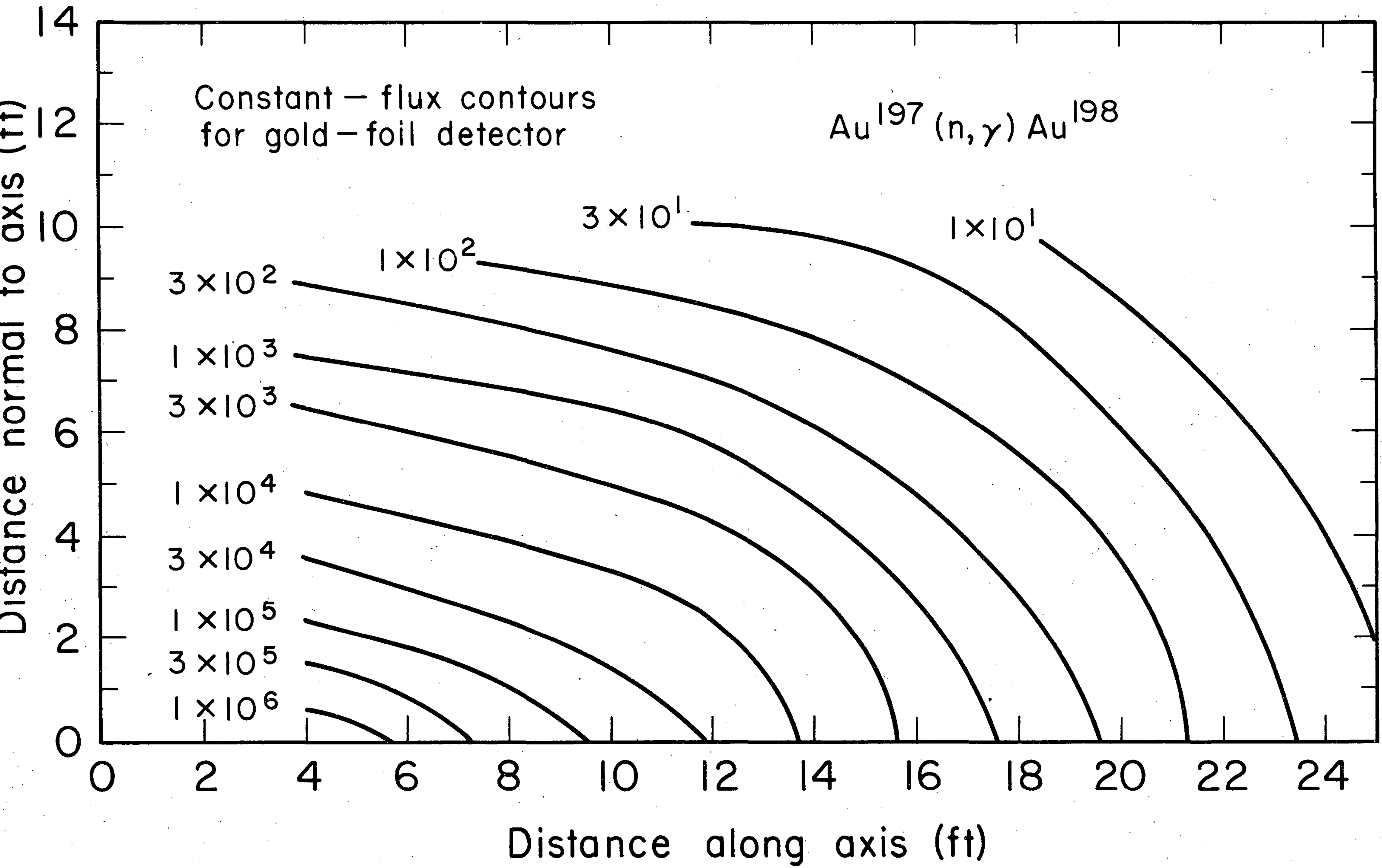

Fig. 7 (a)

MUB-4048

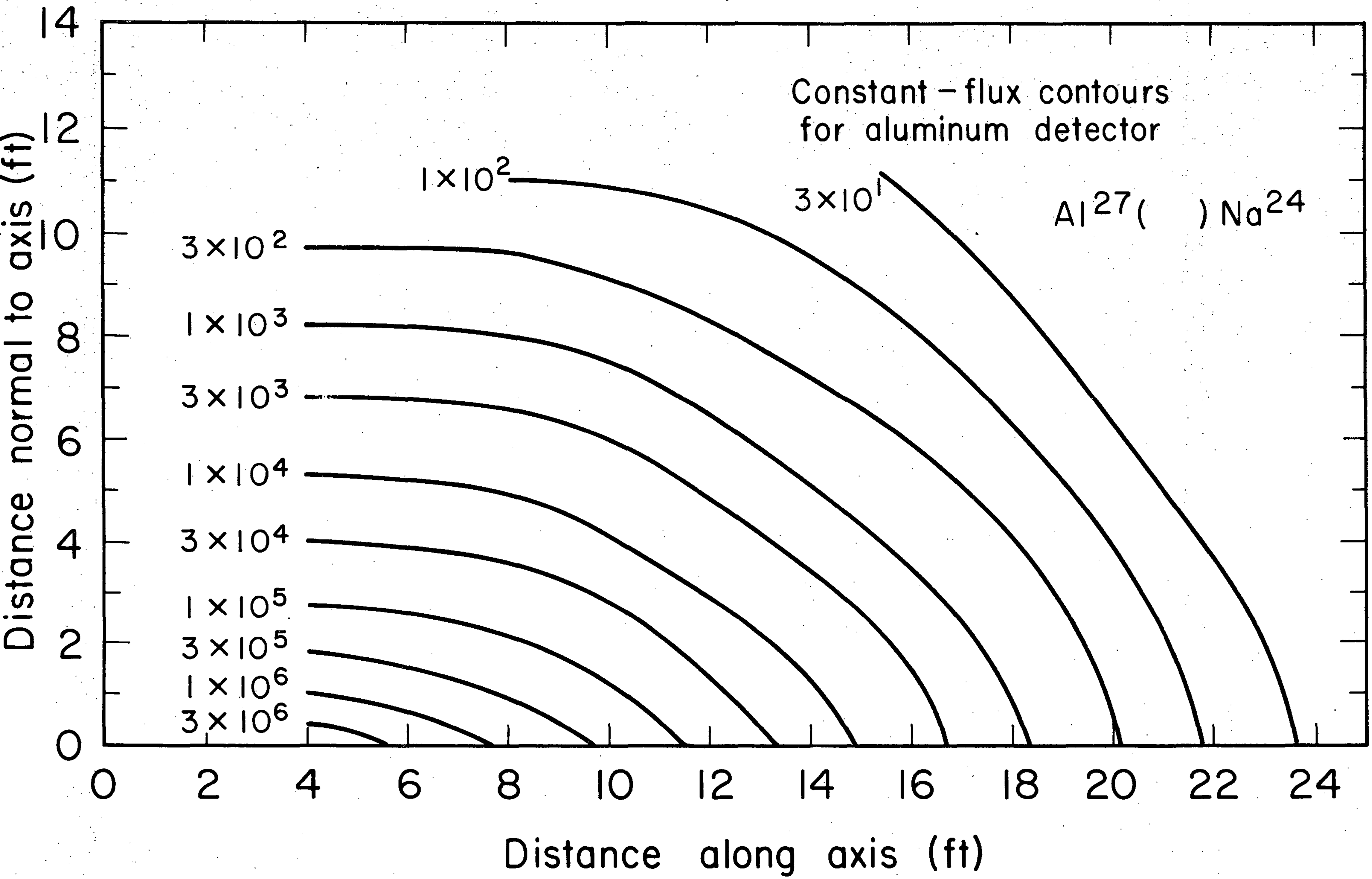

Fig. 7 (b)

MUB-4049

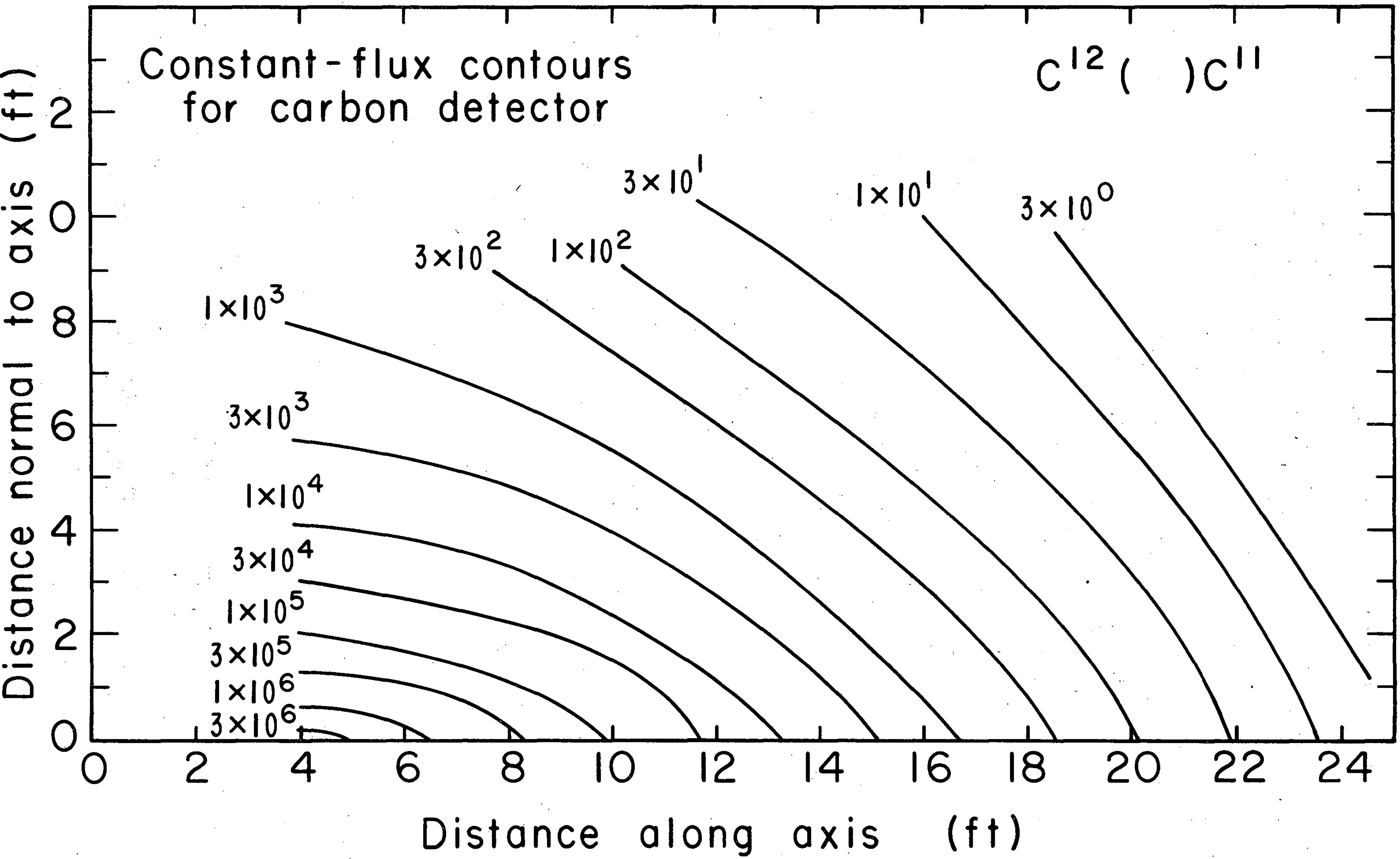

Fig. 7 (c)

MUB-3059 -A

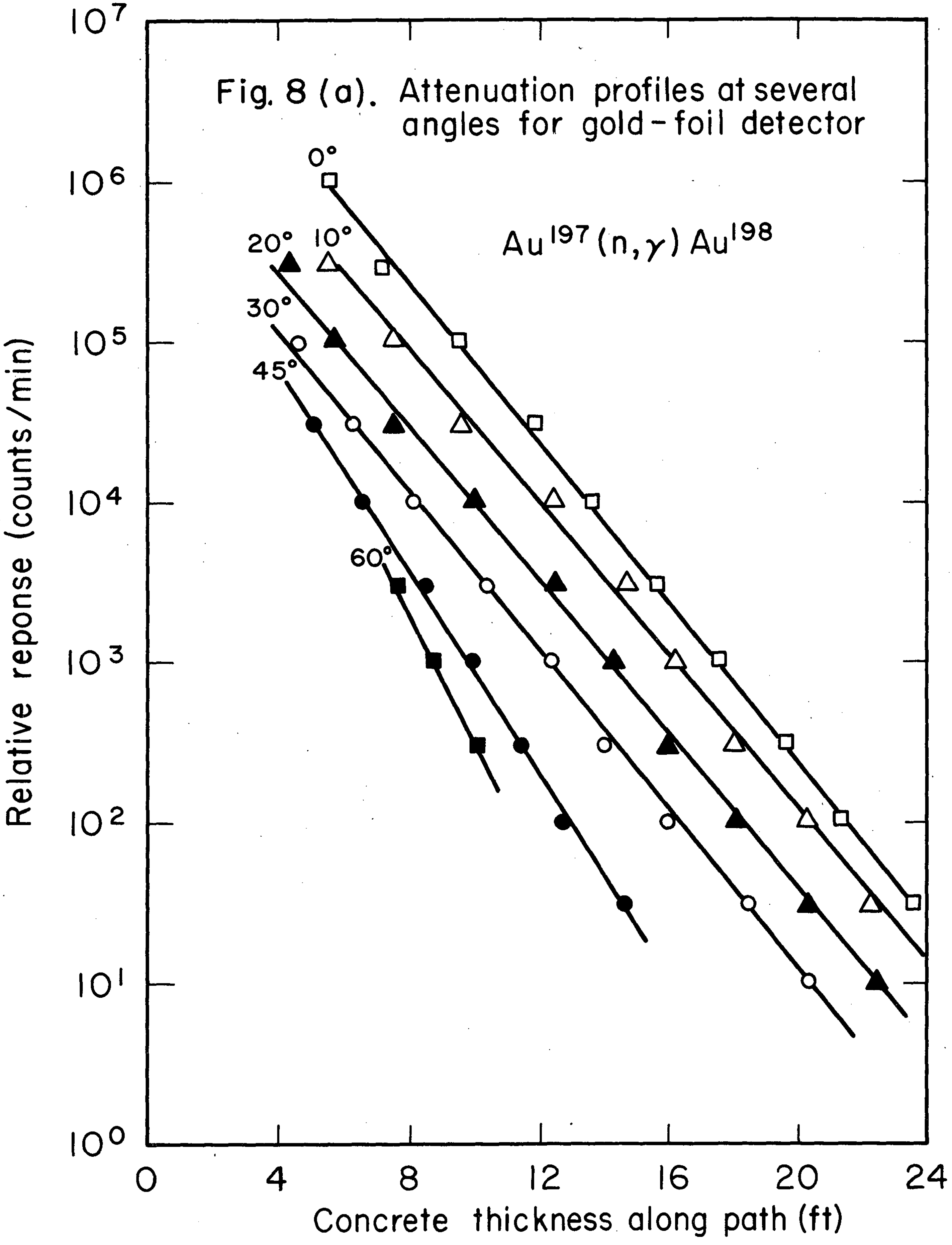

Fig. 8 (a). Attenuation profiles at several angles for gold-foil detector
$Au^{197}(n,\gamma)Au^{198}$
0°
10°
20°
30°
45°
60°
Relative reponse (counts/min)
10^7
10^6
10^5
10^4
10^3
10^2
10^1
10^0
0
4
8
12
16
20
24
Concrete thickness along path (ft)

MUB-4050

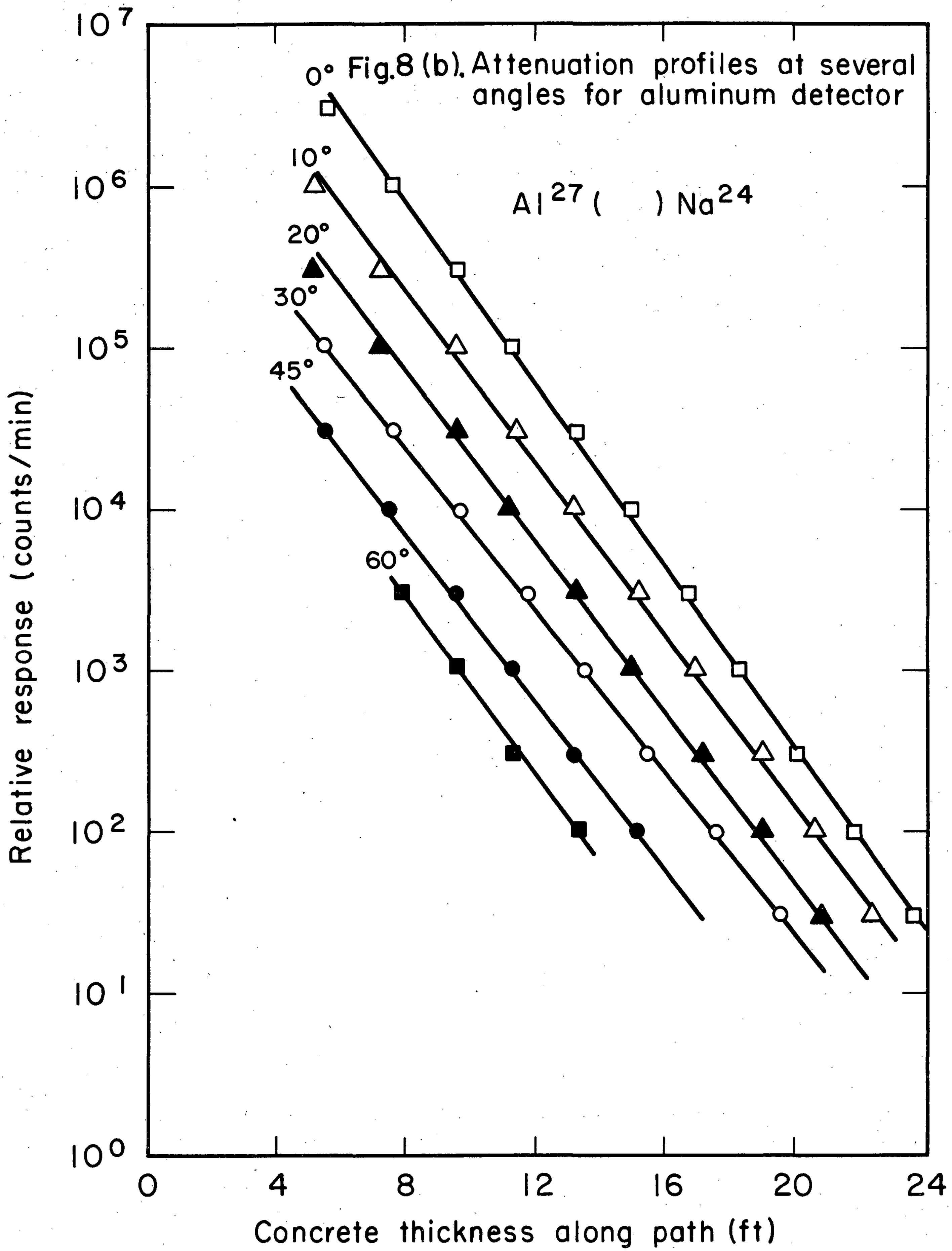

Fig.8 (b). Attenuation profiles at several angles for aluminum detector
Al^{27} (   ) Na^{24}
0°
10°
20°
30°
45°
60°
Relative response (counts/min)
10^7
10^6
10^5
10^4
10^3
10^2
10^1
10^0
Concrete thickness along path (ft)
0
4
8
12
16
20
24

MUB-4051

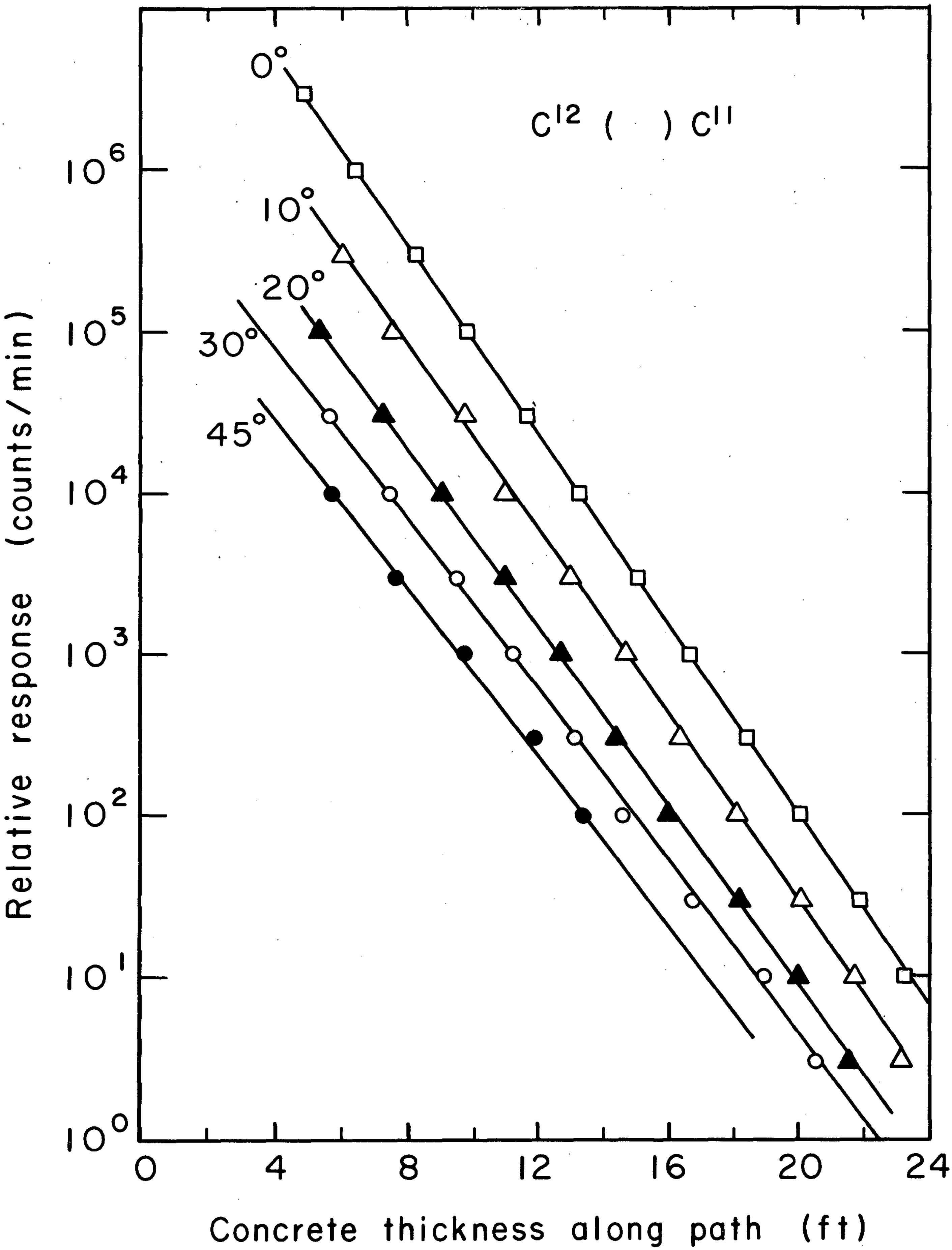

Fig. 8 (c). Attenuation profiles at several angles for carbon detector

MUB-3060 -A

paper, with 10 divisions per centimeter both vertically and horizontally, Keuffel and Esser type 359-14G, or equivalent.

Figures 5 through 8 are sets of triplets, for which we adopt the following convention: gold data are presented as the "a" member; aluminum data are presented as the "b" member; and carbon data are presented as the "c" member. We emphasize characteristics of the radiation field as reported by the carbon scintillators, because this detector has the highest energy threshold in the group and should therefore provide the most meaningful information for shield design. Discussion of these figures is based on the carbon member in each set, and the other detectors will merit discussion when their response differs significantly from carbon data.

RESULTS

Attenuation Measurements

Figure 4 shows attenuation profiles measured along the beam axis for the three detectors. Plotted points are actual data points, normalized to identical activity at the 8-ft position, for ease of comparison. The gold reaction is a thermal-neutron capture, and is also a valid indicator of total fast-neutron flux as used here; the aluminum reaction has a neutron threshold energy of about 6.7 MeV; and the carbon reaction has a neutron threshold energy of about 20.4 MeV. Both aluminum and carbon reactions can be initiated by protons of somewhat higher energies. We see that the slopes of all three curves become similar at great shield depths, but are clearly not identical. We take the carbon curve to be most representative of the high-energy component within the shield. The 1/e attenuation length observed along the straight portion of this curve is 108 g/cm^2, using 2.4 g/cm^3 as the density for ordinary concrete.

Figure 5c shows lateral profiles taken at each 4-ft depth for the carbon detectors. The shield edge is at about 11 ft on the abscissa. Profiles change smoothly from concave upwards near the shield front to convex upwards at great depths. From data taken at the greatest depth, it is evident that we are approaching the condition in which the profiles approximate plane wave fronts. Several simple transformations of this data have been performed; three of these are presented in Figs. 6 through 8.

Figure 6c shows carbon profiles of constant attenuation at lateral positions relative to the intensity along the beam axis normal to each position. Curves show fractional values of beam-axis intensity at off-axis positions. For example, at 16-ft depth, the intensity decreases a factor of 100 at 9 ft off beam axis. Irregularities in Fig. 6a gold profiles are thought to be caused by local inhomogeneities in the thermal neutron-capture properties at such sites.

Figure 7c shows constant-intensity contours existing within the shield array. The values listed with contours are in terms of neutrons/cm^2-sec (or protons/cm^2-sec) for a 6.2-BeV proton beam of about 5×10^8 protons/sec incident on the shield array; the reaction cross section to produce carbon-11 is taken to be 30 mb. Similar normalizations to absolute incident-beam intensity for gold and aluminum detectors are not yet available.

Figure 8 is constructed from the contours presented in Fig. 7. Points plotted on Fig. 8 represent intersections of selected paths through the shield with contours of Fig. 7. The origin for this transformation is taken to be the point at which the beam strikes the front surface of the shield. We plot detector activity versus path length through the array, taking several different angles with respect to the beam line.

Figure 8c shows the resulting attenuation curves for the carbon detector. The upper-most curve, the 0 deg or beam-axis profile, is shown for reference. The four other profiles are, in order downwards, at 10, 20, 30, and 45 deg. The significant feature of these curves is that all slopes are essentially identical. That is, the mean attenuation length appears to be constant for all angles to 45 deg, at all depths beyond about 5 ft, when we measure distance from the point of beam incidence. A reasonable extrapolation of the data indicates that the same attenuation length is observed at an angle of 60 deg.

The aluminum curves of Fig. 8b show the same slope similarity for all angles investigated---to 60 deg. The gold curves of Fig. 8a show the same similarity for all angles through 30 deg, but exhibit increasing slope (more rapid attenuation) at greater angles. Data points for the high-angle profiles lie close to the shield edge, and loss of thermal neutrons by diffusion out of the slots may account for this effect.

Neutron Spectra

Several kinds of useful results were expected from this experiment. We were most interested in the neutron component of the radiation produced and propagated through the shield array, because this component usually determines the shielding requirements for high-energy accelerators. The use of activation-threshold detectors, within the formalism developed by John Ringle of our group,[1] held good promise for obtaining neutron-spectrum information. Briefly, this method is as follows. We determine the induced activations of exposed detectors by using gamma-ray spectrometric analysis. These activations then are used as input data for a digital-computer program. The computer program calculates a neutron spectrum that would have produced the observed activations. The calculation uses detailed cross-section information for each activation reaction, over the energy range 1 to 30 MeV. The use of detailed cross-section data is an important departure from the usual procedure followed in threshold-detector methods.

Bevatron experimental conditions impose two new problems on the neutron-spectrum calculation method. The first of these is the presence of protons with energies capable of initiating some of the activation reactions. The second is the presence of both neutrons and protons with energies far beyond the range for which the method was initially intended. We are now revising the method so that these problem areas will lie within the valid range of the method. It is not yet clear when these efforts will be successful. Consequently, we do not have neutron-spectrum information now.

Accelerator Activation

Another kind of information obtained from our experiment relates to accelerator-activation problems. Several threshold detector elements are also important accelerator construction materials: aluminum, copper, iron, nickel, and perhaps magnesium and titanium. The most prominent gamma-emitting isotopes produced in these elements have been studied continuously by gamma-ray spectroscopy since the irradiation. The observed activities can be related to known irradiation conditions; thus we can estimate realistically the quantities of these activities produced from any given 6.2-BeV proton bombardment. Such information can be used to estimate radiation intensities that would be observed from accelerator structures built of these different materials. We then will have a reasonable grasp of the induced-activity parameter, and can use it along with the usual mechanical and electrical design parameters to help evaluate proposed structural design features.

ADDITIONAL STUDIES AND REPORTS

Several other detector sets employed during this experiment included nuclear emulsions for fast-neutron spectra measurement, nuclear emulsions for study of high-energy cascade phenomena, and sulfur discs for fast-neutron flux measurement. The latter two studies are being conducted jointly by members of the Lawrence Radiation Laboratory and the Rutherford High Energy Physics Laboratory, Harwell, England.

Data analysis is proceeding, both at Berkeley and in Harwell. Our aim is to combine all these results into a comprehensive summary of the experiment, to be published promptly upon completion of data analysis.

SUMMARY

The information learned from these attenuation measurements should be very useful in the design of shielding. Massive backstops, or beam absorbers, for high-intensity external proton beams produced by accelerators like the Bevatron, are a practical necessity. This is a costly necessity, however, in terms of space, time, and money. Our experiment was done with just such a structure, and the results should implement the design of beam absorbers that are more closely matched to the shielding requirements than has been possible in the past. Considerable savings should be realized.

The experiment was done with a sort of "narrow beam" geometry; the results can be transformed to "broad beam" conditions, and then applied to design of general shielding for high-energy accelerators.

ACKNOWLEDGMENTS

Many other people at Berkeley were involved with this experiment, and deserve much credit for the extent of our success. When the complete report of the experiment is written, we will attempt to acknowledge this extensive support in proper detail. In the present context, we express thanks to Dr. B. J. Moyer, H. Wade Patterson, and L. D. Stephens of the Health Physics Department, and to R. Thomas, on leave at Berkeley from the Rutherford Laboratory, with respect to design and execution of the experiment. We thank the Bevatron staff and crew members for providing a beam facility and shield array of such high efficiency for our purposes, also for skillful and competent operation of the accelerator during our experimental runs.

This work was done under the auspices of the U. S. Atomic Energy Commission.

BIBLIOGRAPHY

1. John C. Ringle, A Technique for Measuring Neutron Spectra in the Range 2.5 to 30 MeV Using Threshold Detectors, Lawrence Radiation Laboratory Report UCRL-10732, October 11, 1963.